Since January 2020 Elsevier has created a COVID-19 resource centre with free information in English and Mandarin on the novel coronavirus COVID-19. The COVID-19 resource centre is hosted on Elsevier Connect, the company's public news and information website.

Virology 382 (2008) 239–249

Contents lists available at ScienceDirect

Virology

journal homepage: www.elsevier.com/locate/yviro

Roles for the recycling endosome, Rab8, and Rab11 in hantavirus release from epithelial cells

Regina K. Rowe [a], Jason W. Suszko [a], Andrew Pekosz [a,b,*]

[a] Department of Molecular Microbiology, Washington University in St. Louis School of Medicine, St. Louis, MO 63110, USA
[b] Department of Immunology and Pathology, Washington University in St. Louis School of Medicine, St. Louis, MO 63110, USA

ARTICLE INFO

Article history:
Received 21 July 2008
Returned to author for revision
25 August 2008
Accepted 5 September 2008
Available online 31 October 2008

Keywords:
Hantavirus
Andes virus
Recycling endosome
Golgi
Nucleocapsid

ABSTRACT

Hantavirus structural proteins are believed to localize to intracellular membranes often identified as Golgi membranes, in virus-infected cells. After virus budding into the Golgi luminal space, virus-containing vesicles are transported to the plasma membrane via trafficking pathways that are not well defined. Using the New World hantavirus, Andes virus, we have investigated the role of various Rab proteins in the release of hantavirus particles from infected cells. Rabs 8 and 11 were found to colocalize with Andes virus proteins in virus infected cells and when expressed from cDNA, implicating the recycling endosome as an organelle important for hantavirus infection. Small interfering RNA-mediated downregulation of Rab11a alone or Rab11a and Rab11b together resulted in a decrease in infectious virus particle secretion from infected cells. Downregulation of Rab8a did not alter infectious virus release but reduction of both isoforms did. These data implicate the recycling endosome and the Rab proteins associated with vesicular transport to or from this intracellular organelle as an important pathway for hantavirus trafficking to the plasma membrane.

Introduction

Viruses must target structural proteins and genetic material to a specific location in infected cells for efficient assembly of new particles. After assembly, the virus particles must exit the cell in order to gain access to other susceptible cells or to spread from the infected host. Viruses that assemble at the plasma membrane exit the cell by budding directly into the extracellular milieu. Alternatively, some viruses assemble by budding through intracellular membranes and must then be transported to the plasma membrane – a process called virus egress (Ochsenbauer-Jambor et al., 2001). The assembly of several important human pathogens – hepatitis C virus (Lindenbach and Rice, 2002), rotavirus (LeBouder et al., 2008), herpes simplex virus types 1 and 2 (Mettenleiter, 2004), SARS coronavirus (Ksiazek et al., 2003) and various poxviruses (Moss, 2001; Smith and Law, 2004) – occurs at intracellular membranes, but little is known about the trafficking pathways used to deliver the newly formed viral particles to the plasma membrane (Ksiazek et al., 2003; Lai, 2001; Lindenbach and Rice, 2002; Moss, 2001).

Hantaviruses are members of the *Bunyaviridae* family that are further subdivided into Old World and New World groupings (Schmaljohn and Hjelle, 1997). The Old World hantaviruses are primarily found in Asia and Europe and include Hantaan virus, the causative agent of hemorrhagic fever with renal syndrome (HFRS) (Lee et al., 1978; Schmaljohn and Hjelle, 1997). New world hantaviruses, including Sin Nombre and Andes viruses, are found in North and South America, respectively, and are the causative agents of hantavirus pulmonary syndrome (HPS) (Elliott et al., 1994; Nichol et al., 1993; Toro et al., 1998).

A hantavirus genome consists of three single-stranded, negative-sense RNA segments (Hooper et al., 2001) and the entire replication cycle takes place in the cytoplasm (Hooper et al., 2001) with little cytopathic effects on the infected cell (Hardestam et al., 2005; Meyer and Schmaljohn, 2000; Rowe and Pekosz, 2006). Only four proteins are known to be expressed from the genome — the RNA-dependent RNA polymerase (L), two glycoproteins (G_N and G_C) produced by proteolytic cleavage of a precursor protein, and the nucleocapsid protein (N) (Hooper et al., 2001). The viral proteins and RNA localize to intracellular membranes, believed to be part of the Golgi apparatus, particles then bud into the luminal space and are transported to the plasma membrane via a vesicular trafficking pathway that has not been characterized to date (Goldsmith et al., 1995; Hooper et al., 2001; Ravkov and Compans, 2001; Salanueva et al., 2003; Shi and Elliott, 2002).

RabGTPases (Rabs) are a large family of small molecular weight proteins (Stenmark and Olkkonen, 2001) that are critical mediators of vesicle formation, trafficking, and fusion (Slimane et al., 2003; Zerial and McBride, 2001). Rabs gain their specificity for various membranes

* Corresponding author. Current address: W. Harry Feinstone Department of Molecular Microbiology and Immunology Johns Hopkins University Bloomberg School of Public Health, 615 North Wolfe Street, Suite-E5132, Baltimore, MD 21205, USA. Fax: +1 410 955 0105.
E-mail address: apekosz@jhsph.edu (A. Pekosz).

0042-6822/$ – see front matter © 2008 Elsevier Inc. All rights reserved.
doi:10.1016/j.virol.2008.09.021

through interactions with effector molecules (Grosshans et al., 2006; Pfeffer and Aivazian, 2004) and play key roles in many important vesicular transport pathways, including Golgi to plasma membrane transport (Slimane et al., 2003; Zerial and McBride, 2001).

Rab8 and Rab11 have been shown to be critical in trafficking proteins from the Golgi to plasma membrane (Ang et al., 2003; Chen et al., 1998; Li et al., 1993; Zhang et al., 2005). Rab8 and Rab11 are found at the *trans*-Golgi and the recycling endosome, a post-Golgi compartment that serves as a transport intermediate for some cargo *en route* from the TGN to the plasma membrane (Ang et al., 2004; Chen et al., 1998; Li et al., 1993). Disruption of either Rab8- or Rab11-specific pathways leads to inhibition of recycling endosome-dependent TGN to plasma membrane transport as well as plasma membrane recycling (Ang et al., 2003, 2004; Brock et al., 2003; Chen et al., 1998; Li et al., 1993; Neznanov et al., 2003; Schlierf et al., 2000; Zhang et al., 2005). However, the recycling endosome, Rab8, and Rab11 are not required for trafficking of all proteins from the TGN to plasma membrane as plasma membrane delivery of the Influenza A virus hemagglutinin protein is unaffected by inhibition of Rab8 or Rab11 trafficking pathways (Chen et al., 1998; Li et al., 1993; Yoshimori et al., 1996). This indicates that specific sorting events occur to direct cargo into multiple transport pathways (i.e. recycling endosome-dependent and independent) to facilitate delivery from the TGN to the plasma membrane.

Viruses often hijack existing cellular pathways in order to complete various stages of their life cycle. We investigated the vesicular trafficking pathways important for ANDV release from infected cells and describe a role for the recycling endosome, and specifically Rab8 and Rab11, during ANDV exit from non-polarized epithelial cells.

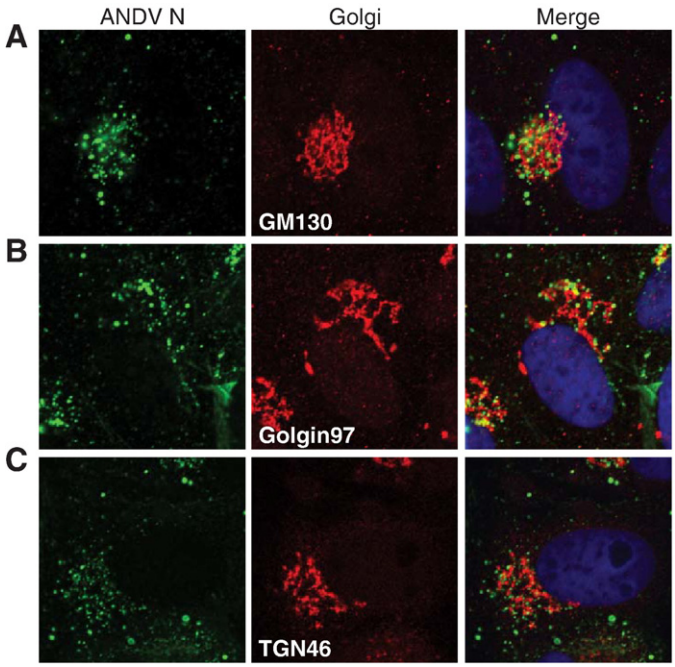

Fig. 1. ANDV N partially localizes to the Golgi and *trans*-Golgi during infection. Vero cells were infected with ANDV and fixed for immunofluorescence at 2 dpi. Cells were immunostained for ANDV N (green, Alexa Fluor 488) and the following Golgi and *trans*-Golgi markers (red, Alexa Fluor 555) (A) GM130, (B) Golgin97, and (C) TGN46. Cells were visualized using confocal microscopy. Nuclei (blue) were counterstained with TO-PRO-3 and are shown in the merged panels only. All images are confocal single planes acquired at a 63× optical magnification and 3× digital zoom.

Results

ANDV N forms cytoplasmic inclusions and localizes to intracellular vesicular membranes

Viruses in the family *Bunyaviridae* are thought to primarily assemble at membranes of the Golgi and *trans*-Golgi network (TGN) and these cellular compartments likely play a critical role in ANDV replication and assembly. We focused our studies on the nucleocapsid protein because it is the most abundant protein in the virion (Kaukinen et al., 2005) and localizes to the site of viral RNA replication and particle assembly (Goldsmith et al., 1995; Hooper et al., 2001; Ravkov and Compans, 2001). While the ANDV glycoproteins have been shown to localize to the Golgi and TGN during infection and from cDNA expression (Deyde et al., 2005), little is known about the localization of ANDV N with this compartment. To determine the intracellular localization of ANDV N during infection, immunofluorescence confocal microscopy was performed on ANDV-infected Vero cells immunostained for ANDV N and various markers of the Golgi and TGN (Fig. 1). ANDV N showed partial overlap with GM130, Golgin-97 and TGN46, however the extent of colocalization differed slightly. The greatest degree of colocalization was observed with GM130 (Fig. 1A), a protein associated with the *cis*-Golgi (Pfeffer, 2001). Less colocalization was observed with Golgin97 (Fig. 1B), a membrane-associated protein of the TGN (Gu et al., 2001; Yoshino et al., 2003). ANDV N consistently showed more colocalization with membranes positive for TGN46 (Fig. 1C) than membranes positive for Golgin97. TGN46 is an integral membrane protein that recycles between the plasma membrane and TGN, but the recycling kinetics result in TGN enrichment (Greaves and Chamberlain, 2007; Roquemore and Banting, 1998). While there was only partial overlap of ANDV N with the Golgi markers, the remaining ANDV N was consistently in close proximity to all of the Golgi markers, suggesting a close spatial relationship between nucleocapsid and the Golgi. This data indicates that while a portion of ANDV N does localize with Golgi and TGN membranes, the majority of the protein appears to be proximal but not associated with these membrane compartments.

To gain additional insights on the location of ANDV N during infection, immuno-electron microscopy was performed on ANDV-infected cells (Fig. 2). ANDV N was localized throughout the cytoplasm but concentrated in the perinuclear region (Fig. 2). ANDV N was primarily localized to large, granulofilamentous structures surrounded by large numbers of mitochondria (Figs. 2A and B). These structures were not membrane-bound, but were proximal to intracellular membranes resembling Golgi cisternae (Fig. 2C). Smaller accumulations of ANDV N, not in filamentous structures, also localized to the membranes of small vesicles in close proximity to the Golgi (Figs. 2C and D). Additionally, the structure of the Golgi was altered, with extensive small vesicles surrounding the cisternae (Figs. 2C and D). There was no ANDV N found present at the plasma membrane or enclosed within membrane structures (~75 cells observed, data not shown), and even with large amounts of ANDV N present in the infected cells, no obvious structures resembling viral particles were detected. This data suggests that there are two cellular pools of ANDV N, one that is present in large, granulofilamentous structures not significantly associated with membranes and one that is membrane-associated.

ANDV N colocalizes with Rabs of the recycling endosome

In order to determine the role of various cellular trafficking pathways in ANDV replication we focused our remaining studies on the portion of ANDV N localized to intracellular vesicular membranes. ANDV N is predicted to be a peripheral membrane protein that exists in a dynamic equilibrium between membrane bound and cytosolic pools (Hooper et al., 2001; Kaukinen et al., 2005; Ravkov and Compans, 2001). To identify specific vesicular populations during infection, ANDV-infected cells were transfected with cDNAs encoding eGFP-fusion proteins associated with various host cell trafficking pathways and analyzed by confocal microscopy for colocalization of

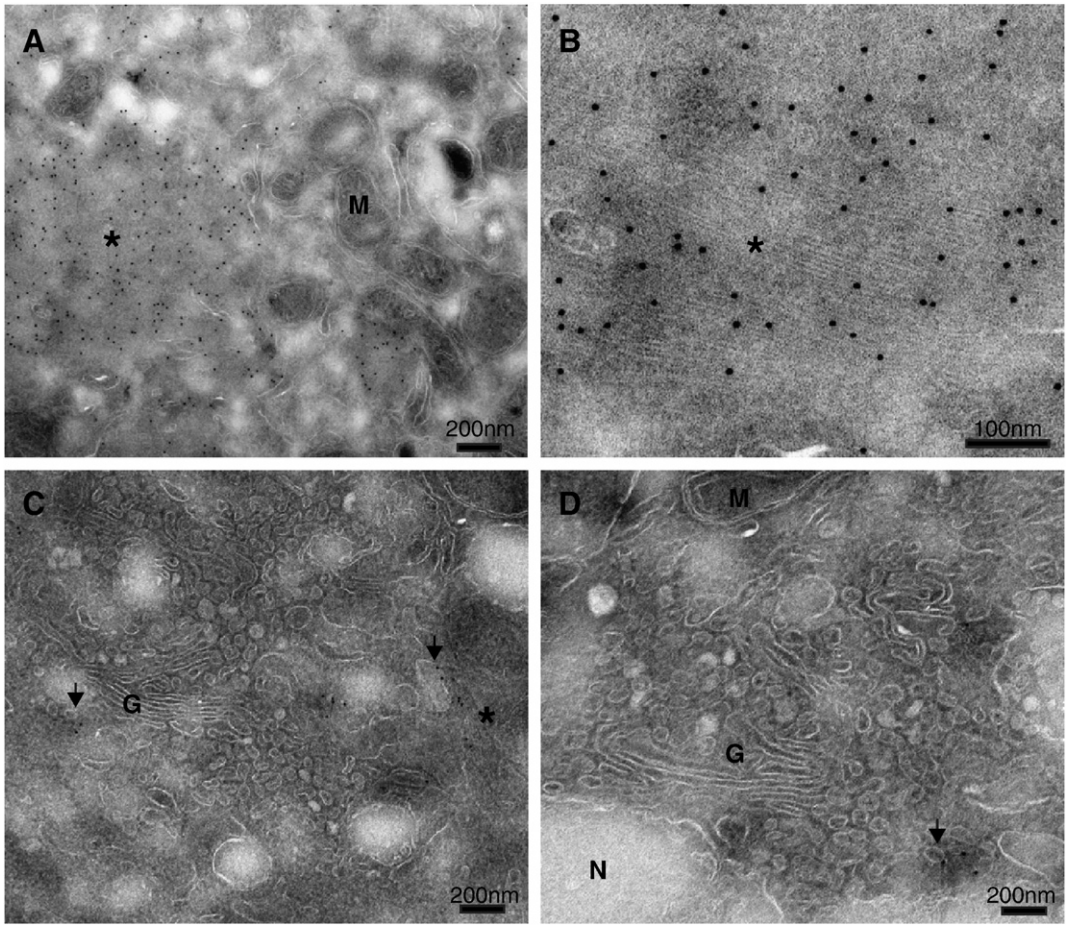

Fig. 2. Ultrastructural analysis of ANDV N during infection by immunoelectron microscopy. At 2 d (A and B) and 4 d (C and D) post infection, ANDV-infected Vero cells were and immunolabeled using ANDV N-specific rat immunesera followed by secondary antibody conjugated to 12 nm colloidal gold particles. Granulofilamentous structures are indicated with an asterisk (*), while vesicle-associated ANDV N is noted by arrowheads. Cellular structures are denoted as follows: mitochondria (M), Golgi (G), and nucleus (N). Scale bars represent 100 or 200 nm as indicated. The image in panel (B) is a cropped and digital zoom of a region in panel (A), and was performed using Adobe Photoshop.

eGFP with ANDV N protein. Using 3-D reconstructions of serial Z-stack images acquired by confocal microscopy (data not shown) we were able to focus on the portion of membrane-associated ANDV N in infected cells expressing cDNAs of proteins associated with various vesicular transport pathways. ANDV-infected cells expressing eGFP-Rab 8 (Fig. 3A) or eGFP-Rab11 (Fig. 3B) show a high degree of colocalization between ANDV N and either Rab protein. We measured the degree of colocalization using parameters within the Volocity software that allowed us to focus on the viral antigen that was associated with the vesicular trafficking proteins (described in the Materials and methods). The percent of eGFP colocalizing with ANDV N was determined by dividing the total colocalization volume by the volume of eGFP, and expressed as percent colocalization (Fig. 3C). Using this calculation, Rab8 and Rab11 had the highest level of colocalization with ANDV N, with 30.1% and 29.2% of the eGFP-Rab proteins colocalizing with ANDV N, respectively. Rabs associated with early endosomes (eGFP-Rab5a), late endosomes (eGFP-Rab7), and late endosomes/lysosomes (Rab9) showed colocalization that was clearly less than that observed with eGFP-Rab8 and eGFP-Rab11. Proteins associated with the multivesicular bodies (CD63-eGFP and eGFP-Vps4A) showed limited colocalization (Fig. 3C). Taken together, these results suggest that the recycling endosome-associated Rabs 8 and 11 colocalize with ANDV N and therefore may play a role in ANDV replication.

Many viral proteins show similar subcellular localization during infection and when expressed independently from cDNA. In order to determine if viral proteins colocalized with Rab8 and Rab11 when expressed from cDNA, Vero cells were transfected with cDNAs expressing either ANDV N (Supplemental Figs. 1A and D) or the ANDV glycoprotein ORF (M), which expresses both G_N and G_C (Supplemental Figs. 1B and E), with either eGFP-Rab8 (Supplemental Figs. 1A and B) or eGFP-Rab11 (Supplemental Figs. 1D and E). Cells were then immunostained for either ANDV N or ANDV glycoproteins and analyzed by confocal microscopy. ANDV N and the ANDV glycoproteins colocalized with eGFP-Rab8 and eGFP-Rab11, suggesting that both proteins can localize to cellular membranes enriched in Rab8 and Rab11 independently of virus infection. The vesicular stomatitis virus G (VSV G) protein has been shown to traffic from the Golgi to the plasma membrane via Rab8- (Ang et al., 2003, 2004; Li et al., 1993) and Rab11-dependent pathways (Chen et al., 1998). As expected, VSV G colocalized extensively with both eGFP-Rab8 and eGFP-Rab11 (Supplemental Figs. 1C and F).

ANDV N colocalizes with endogenous Rab8 and Rab11 during infection

The data in Fig. 3 indicated that ANDV N could localize to cellular membranes containing cDNA expressed eGFP-Rab8 or eGFP-Rab11. To determine if the ANDV N colocalized with the endogenous forms of Rab8 and Rab11, mock- or ANDV-infected Vero cells were immunostained at 3 dpi for ANDV N and either endogenous Rab8 (Fig. 4A) or Rab11 (Fig. 4B). The signal intensity for immunostaining of endogenous Rabs was lower when compared to the cDNA-expressed eGFP proteins — most likely a combination of higher expression levels of the plasmid expressed fusion proteins and the intense fluorescence signal

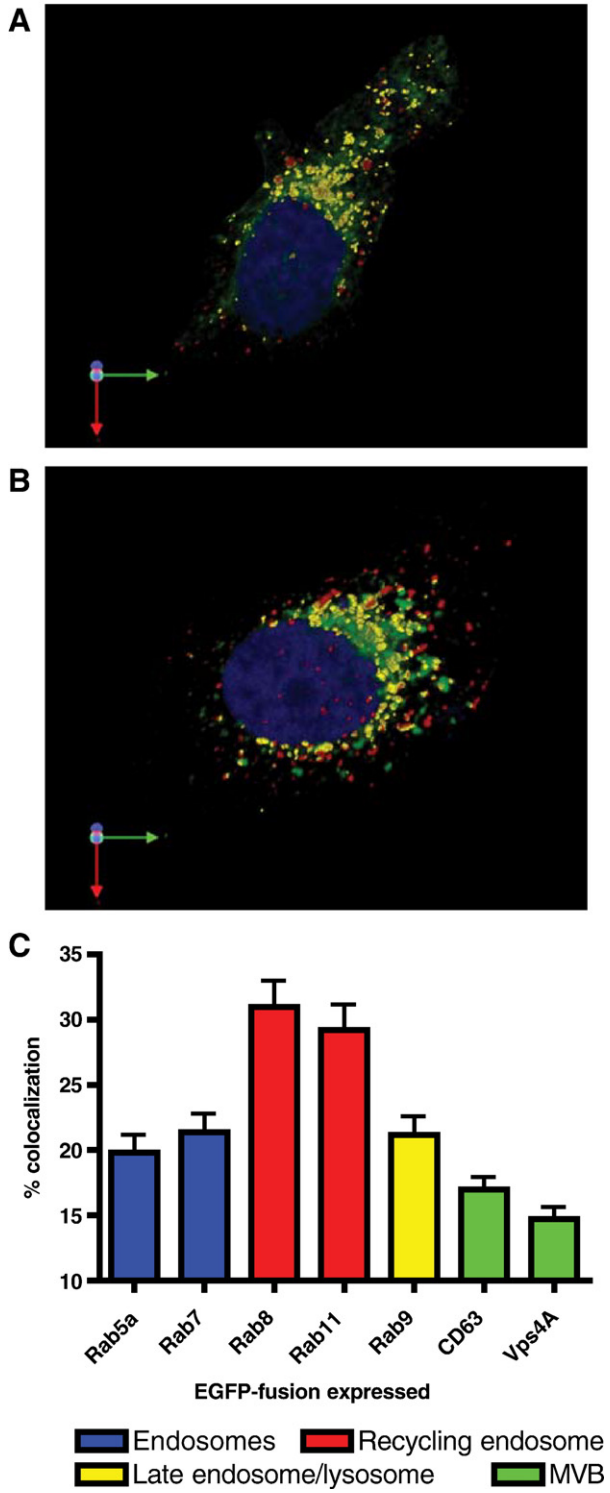

Fig. 3. ANDV N localizes to the recycling endosome and has little colocalization with proteins of other vesicular trafficking pathways. (A and B) Vero cells were infected with ANDV, then transfected at 3 dpi with cDNAs expressing (A) eGFP-Rab8 or (B) eGFP-Rab11 fusion proteins (green). Cells were fixed 18 hpt, immunostained for ANDV N (red, AlexaFluor 594), counterstained for the nucleus with TO-PRO-3 (blue), and visualized using confocal microscopy. 3-D reconstructions were created from confocal z-stacks using the Improvision Volocity imaging software. The regions of colocalization between eGFP and ANDV N can be seen in yellow. (C) 3-D regions of colocalization between ANDV N and eGFP-fusion proteins were measured as described in the Materials and methods. The volume of colocalization was normalized to the volume of eGFP and expressed as percent colocalization. The trafficking molecules were grouped into the following trafficking pathways: endosome (blue bars), recycling endosome (red bars), late endosome/lysosome (yellow bars), and multvesicular body (MVB, green bars). Data presented is the mean of four independent experiments and at least 5 cells per cDNA transfection in each experiment.

of eGFP. While endogenous Rab8 was readily detectable, endogenous Rab11 consistently showed low fluorescent intensity (compare green fluorescence images in Fig. 4). Despite the low level of signal intensity there were notable regions of colocalization between ANDV N and both Rab8 (Fig. 4a) and Rab11 (Fig. 4b), suggesting that a portion of ANDV N expressed during infection was present at membranes containing Rab8 and Rab11 and providing further support for a role for Rab8 and Rab11 during ANDV infection. ANDV N protein also colocalized with fluorescently labeled transferrin (data not shown), further supporting a role for the recycling endosome in ANDV infection.

Dominant negative and constitutively active forms of Rab11 have altered levels of colocalization with ANDV N during infection

Amino acid substitutions at highly conserved residues within RabGTPases create proteins that are no longer capable of GDP–GTP cycling. A serine to asparagine mutation at position 25 (S25N) in Rab11 results in constitutive binding of GDP and locks the protein in a dominant negative form. In contrast, a glutamine to lysine mutation at position 70 (Q70L) prevents GTP hydrolysis, resulting in a constitutively active protein. The analogous mutations in Rab8 are T22N and Q70L. These mutant proteins often display altered subcellular localization due to augmented protein–protein interactions (Chen et al., 1998; Hattula et al., 2006; Ren et al., 1998; Scheiffele et al., 1995). To determine if expression of mutated eGFP-Rab8 and -Rab11 proteins during ANDV infection altered the colocalization of these proteins with ANDV N, infected Vero cells were transfected with cDNAs expressing eGFP-fusions of either wild-type, dominant negative (GDP-bound), or constitutively active (GTP-bound) mutants of eGFP-Rab8 and 11 (Fig. 5). There were notable differences in the subcellular distribution of the eGFP-Rab8 proteins. The GDP-bound form (Rab8T22N) had a tighter perinuclear localization and fewer effects on cell morphology (Fig. 5B), while the GTP-bound protein (Rab8Q67L, Fig. 5C) had an expression pattern similar to wild-type eGFP-Rab8 (Fig. 5A) (Hattula et al., 2006; Scheiffele et al., 1995). Interestingly, both forms of eGFP-Rab8 displayed similar levels of colocalization with ANDV N compared to wild-type Rab8 (Figs. 5A–C, quantitated data in Fig. 5D). In contrast, eGFP-Rab11S25N showed increased levels of colocalization with ANDV N while the constitutively active eGFP-Rab11Q70L showed an approximately 50% decrease in colocalization when compared to eGFP-Rab11 (Figs. 5E–G, quantitated data in Fig. 5H).

Rab11 has been reported to function in trafficking between the *trans*-Golgi and recycling endosome, therefore, we determined the localization of the eGFP-Rab11 proteins with respect to the *trans*-Golgi marker, TGN46 (Fig. 6). Wild-type eGFP-Rab11 showed partial localization with TGN46 (Fig. 6A), while the Q70L mutant showed limited overlap (Fig. 6C). In contrast, the membrane-associated portion of Rab11S25N showed almost complete localization with TGN46 (Fig. 6B). These data are consistent with previous reports that the dominant negative Rab11 localizes to the TGN, while the constitutive active form localizes at the recycling endosome (Chen et al., 1998; Neznanov et al., 2003).

siRNA-mediated downregulation of Rab8 and Rab11 block ANDV secretion

To determine if Rabs 8 and 11 played a functional role in ANDV release from infected cells, RNA interference (RNAi) (Elbashir et al., 2001) was utilized to downregulate Rab8 and Rab11 protein expression during infection. Many cell surface receptors, including the hantavirus receptor β3 integrin, are recycled through the recycling endosome (Jones et al., 2006), therefore downregulation of molecules within this pathway could alter surface expression of the viral receptor, thus affecting virus entry. To avoid altering early

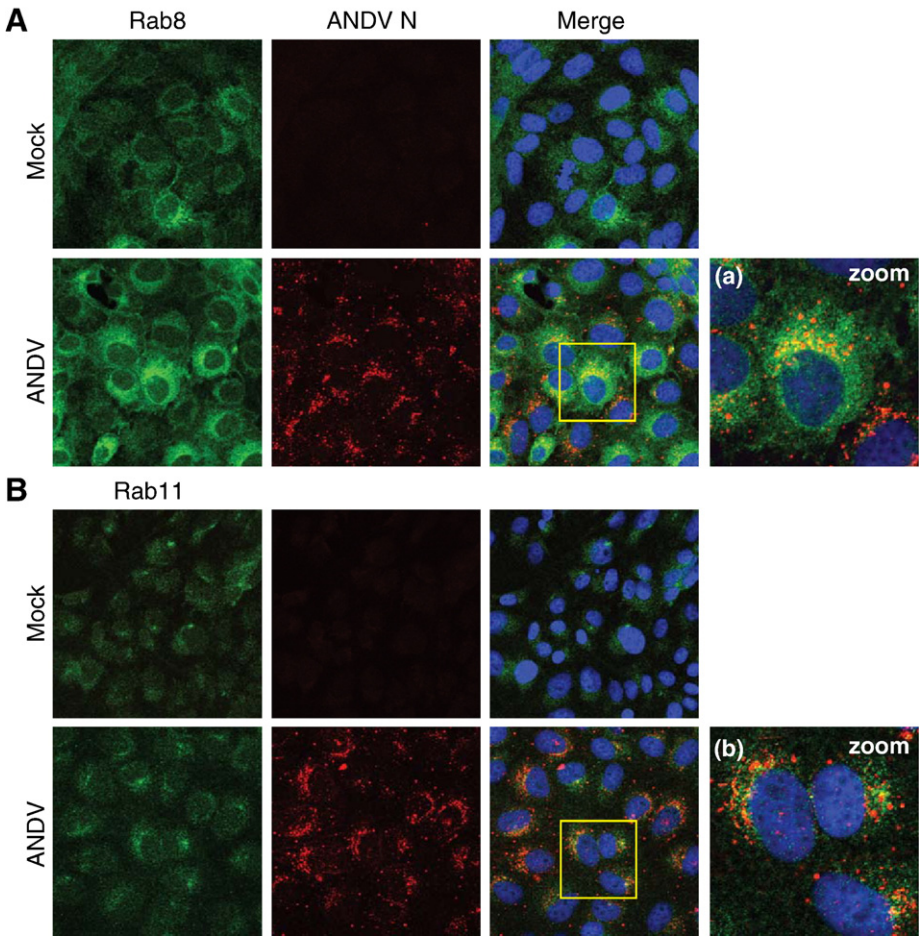

Fig. 4. ANDV N colocalizes with endogenous Rab8 and Rab11 during infection. Mock- or ANDV-infected Vero cells were fixed at 3 dpi and immunostained for ANDV N (red, AlexaFluor 594) and either (A) Rab8 (green, AlexaFluor 488) or (B) Rab11 (green, AlexaFluor 488). Nuclei were counterstained with TO-PRO-3 (blue) and are shown in the merged images only. All images were acquired at 63× magnification. Digital zoom (2×) images of the boxed area in the merged panels for (a) Rab8 and (b) Rab11 are also shown.

events in the virus life cycle, we took advantage of the fact that ANDV infection of Vero cells leads to prolonged, low level virus secretion with little obvious cytopathic effects (Hardestam et al., 2005; Meyer and Schmaljohn, 2000; Rowe and Pekosz, 2006). Seventy-two hours following ANDV infection, Vero cells were transfected with siRNAs specific for the a or b isoforms of Rabs 8 and 11, along with siRNA controls. At this time, over 90% of the cells are expressing viral antigen (data not shown). Since most cells express two isoforms (a and b) of Rab8 and Rab11 (Lai et al., 1994; Lau and Mruk, 2003), we utilized pooled siRNAs specific for either the a isoform or both the a and b isoforms. Four siRNAs per target transcript were used. At 48 hpt, there was a significant decrease in the Rab8 protein expression levels (Fig. 7A) after transfection with siRNAs targeting Rab8a (52.7% decrease) or both Rab8a and 8b isoforms (51.6% decrease). Transfection of siRNAs specific for Rab11a or Rab11a and 11b isoforms, as well as transfection reagent alone (siQst) resulted in no changes in Rab8 expression levels (Fig. 7A). There was also a significant decrease in the Rab11 protein expression levels (Fig. 7A) after transfection with siRNAs targeting Rab11a (78.1% decrease) or both Rab11a and 11b isoforms (61.9% decrease), again with no off-target effects from siRNAs targeting Rab8 isoforms. Unfortunately, the antibodies used cannot distinguish between the two isoforms, so we could not determine the specific downregulation of the b isoforms. Downregulation of all four targets (Rab8a and 8b, Rab11a and 11b) resulted in significant decreases in both Rab8 (48.8% decrease) and Rab11 (61.3% decrease) proteins (Fig. 7A). The level of β-actin expression was not altered after any siRNA transfection (Fig. 7A). The treatment of cells with structured, double stranded RNAs can lead to host cell antiviral responses that can inhibit viral replication (Stetson and Medzhitov, 2006). Intracellular ANDV N levels remained constant after siRNA transfection (Fig. 7B), indicating there were no adverse effects of siRNA transfection on viral protein production.

In order to assess if siRNA treatments altered the secretion of infectious virus particles, infected-cell supernatants were harvested immediately before and 48 h after siRNA transfection. Infectious virus production was quantified by an immune $TCID_{50}$ assay and expressed as a fold decrease in virus production (Fig. 7C). Downregulation of Rab11a or Rab11a and 11b resulted in a nearly 10 fold decrease in virus secretion, indicating Rab11 isoforms were functionally important for ANDV release from infected cells. Transfection with control siRNAs (siQst, transfection reagent alone; siGlo, RISC-binding deficient siRNA; and murine PKR siRNA, a protein not associated with vesicular transport) did not alter the amount of infectious virus production when compared to mock-transfected cells, indicating there were no non-specific effects of siRNA transfection on ANDV virus production. Interestingly, siRNAs specific for Rab8a did not alter ANDV virus secretion (Fig. 7C) even though Rab8 levels were decreased significantly (Fig. 7A). However, downregulation of both Rab8a and 8b led to a 10-fold decrease in virus secretion. Decreasing all four Rab isoforms did not enhance the decrease virus secretion compared to downregulating Rab8a/b, Rab11a, or Rab11a/b. The data in Fig. 7 demonstrates that Rabs associated with the recycling endosome play a functional role in ANDV secretion from epithelial cells, and

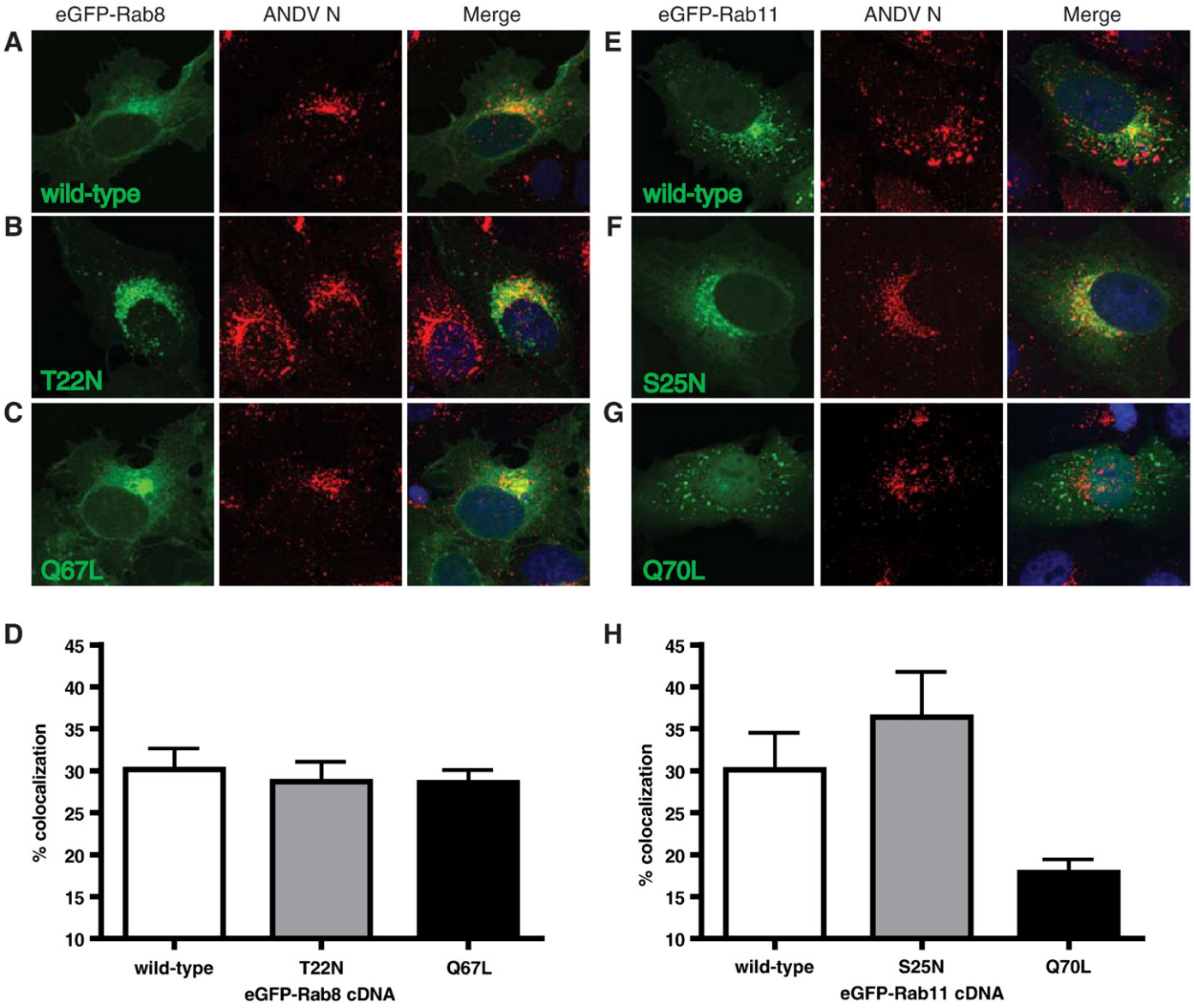

Fig. 5. Dominant negative and constitutively active forms of Rab11 have altered levels of colocalization with ANDV N during infection. ANDV-infected Vero cells were transfected with cDNAs expressing (A) wild-type, (B) T22N mutant, GDP-bound dominant negative, and (C) Q67L mutant, GTP-bound constitutively active, forms of eGFP-Rab8 (green); and (E) wild-type, (F) S25N mutant, GDP-bound dominant negative, and (G) Q70L mutant, GTP-bound constitutively active, forms of eGFP-Rab11 (green). At 18 hpt, cells were fixed and immunostained for ANDV N (red, AlexaFluor 555). Nuclei were counterstained with TO-PRO-3 (blue) and are shown in the merged images only. All images are flattened reconstructions of confocal z-stacks acquired at 63× optical magnification and 2× digital zoom. Levels of colocalization between ANDV N and (D) eGFP-Rab8 and (H) eGFP-Rab11 proteins were quantitated using the Volocity imaging software. Data presented is the mean of three independent experiments and at least 5 cells per cDNA transfection in each experiment.

specifically indicates Rab11a as a major host cell factor involved in this process.

Discussion

Many viruses in the family *Bunyaviridae* assemble at Golgi membranes and new particles are transported to the plasma membrane via vesicular transport (Nichol, 2001; Salanueva et al., 2003). The vesicular trafficking mechanism utilized during hantavirus egress is poorly understood but the data presented in this study suggests trafficking through the recycling endosome may be a key step in this process for ANDV.

The nucleocapsid proteins of viruses within *Bunyaviridae* have been localized to multiple intracellular compartments. The nucleocapsids of Uukuniemi virus (genus *Phlebovirus*) and Black Creek Canal virus (BCCV, genus *Hantavirus*) have both been shown to localize to Golgi membranes (Jantti et al., 1997; Kuismanen et al., 1982; Ravkov and Compans, 2001). In contrast, Hantaan virus (genus *Hantavirus*) and LaCrosse virus (genus *Orthobunyavirus*) nucleocapsids have been shown to localize to membranes of the endoplasmic reticulum (ER) and ER-Golgi intermediate compartment (ERGIC) (Ramanathan et al., 2007; Stertz et al., 2006). Even though ANDV N had partial colocalization with Golgi and *trans*-Golgi markers by immunofluorescence confocal microscopy, a significant portion did not overlap with these markers. Electron microscopy studies further indicated two populations of nucleocapsid. The majority of ANDV N was localized to large cytoplasmic structures not obviously associated with membranes, which have been previously described as inclusion bodies in studies of other hantaviruses (Goldsmith et al., 1995; Hung et al., 1985; Ravkov et al., 1997). These structures may be caused by accumulation

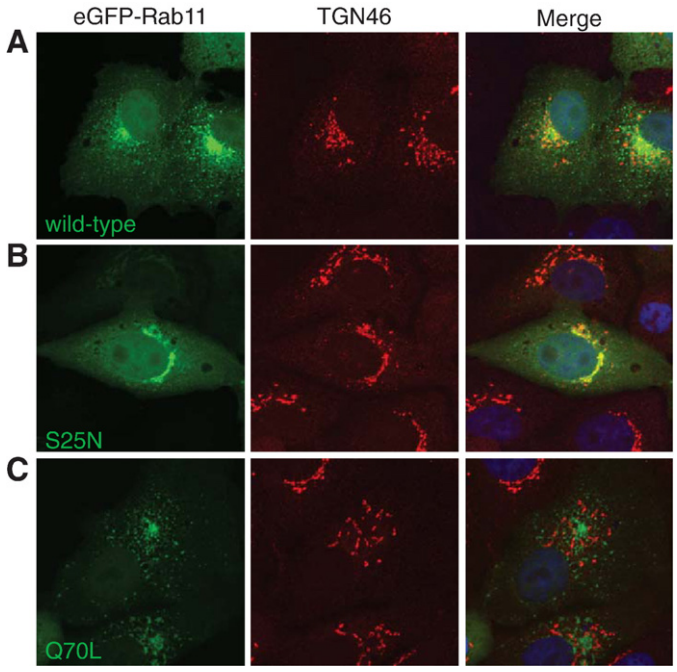

Fig. 6. Dominant negative and constitutively active forms of Rab11 localize to distinct membrane compartments. Vero cells were transfected with cDNAs expressing eGFP-Rab11 (A) wild-type, (B) S25N, or (C) Q70L proteins (green). At 18 hpt, cells were fixed and immunostained for the *trans*-Golgi marker, TGN46 (red, AlexaFluor 594). Nuclei were counterstained with TO-PRO-3 (blue) and are shown in the merged images only. All images are flattened reconstructions of confocal z-stacks acquired at 63× optical magnification and 2× digital zoom.

of large amounts of N protein in infected cells or may be the site of RNA replication as described for the orthobunyavirus, Bunyamwera (Yan et al., 2002). Further studies will be required to determine the composition of these structures. A smaller portion of ANDV N was membrane-associated at vesicles proximal to the Golgi, which has been described for Uukuniemi virus N (Jantti et al., 1997). These vesicles could be part of the Golgi, *trans*-Golgi network, or post-Golgi secretory pathway. In order to identify these vesicles, we focused on proteins involved in host cell vesicular trafficking pathways. From these studies, the data suggests an involvement of the recycling endosome pathway and RabGTPases, Rab8 and Rab11, in ANDV release from infected cells.

Plasma membrane assembly has been noted for Sin Nombre virus (SNV) and BCCV, two New World hantaviruses (Goldsmith et al., 1995; Ravkov et al., 1997), however the lack of plasma membrane localization of ANDV N in the electron microscopy studies strongly suggests limited plasma membrane assembly. However, we could not confirm the site of ANDV assembly because no obvious structures resembling viral particles were observed by electron microscopy at high frequency. This is, perhaps, not surprising given the low numbers of ANDV particles released per cell. It may also be possible that the anti-nucleocapsid sera may not recognize ribonucleocapsids (RNPs) present in budding particles and fully assembled virions. However, based on the localization of ANDV proteins, it is likely that ANDV assembles at membranes of the Golgi or *trans*-Golgi, similar to that observed for Hantaan virus and other viruses in *Bunyaviridae* (Chen et al., 1991; Hung et al., 1985; Kuismanen et al., 1982; Salanueva et al., 2003; Tao et al., 1987).

Our proposed model of ANDV assembly and egress starts with ANDV protein concentrated at the site of assembly to form new particles by budding into the host cell membrane, which is enriched in Rab8 and Rab11 thereby, facilitating the access of newly formed particles to the correct egress trafficking pathway. Egress could then occur via a Rab8- and/or Rab11-mediated mechanism which traffics virus-containing vesicles to the recycling endosome. The virus particles could then be sorted into vesicles destined for the apical or basolateral plasma membrane. It is important to note that our studies utilized non-polarized Vero cells. Intracellular trafficking in polarized versus non-polarized cells may utilize slightly different pathways so an analysis of ANDV trafficking in other relevant cell types (e.g. polarized epithelial cells, macrophages, endothelial cells) is warranted.

The recycling endosome regulates plasma membrane recycling of many cell surface receptors, such as transferrin (Ang et al., 2004; Ren et al., 1998; Schlierf et al., 2000; Sheff et al., 2002), low-density

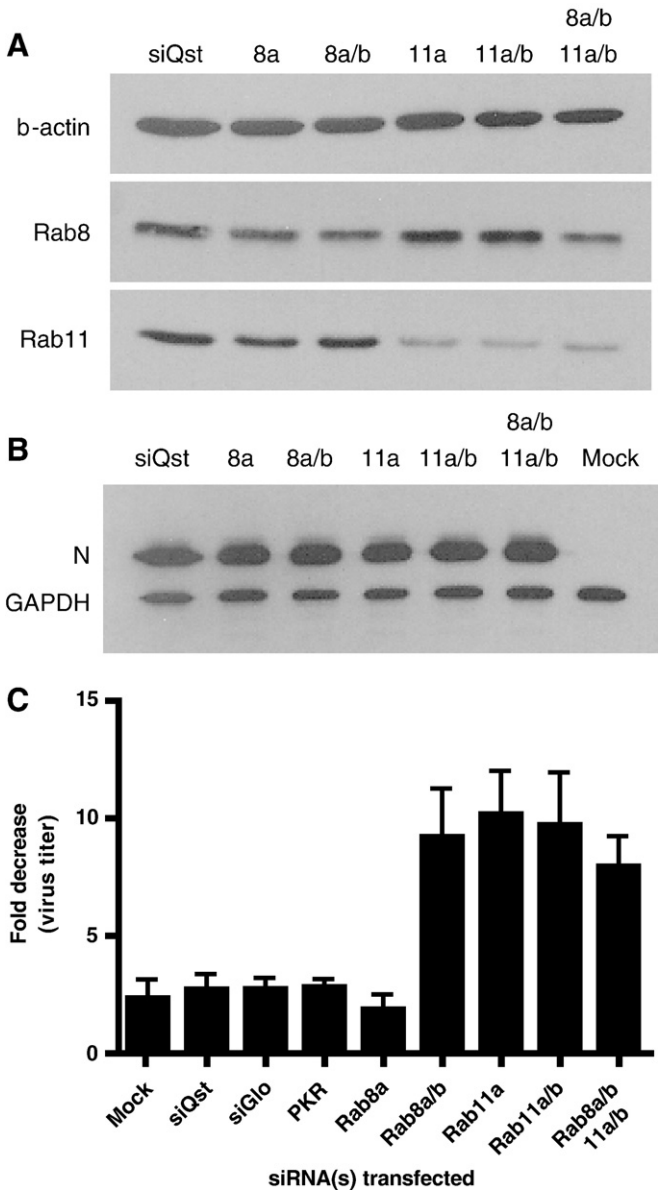

Fig. 7. siRNA downregulation of Rabs of the recycling endosome block ANDV egress. Vero cells were infected with ANDV and at 3 dpi were transfected with the following siRNAs: siGlo (100 nM, RISC-binding deficient siRNA), murine PKR (100 nM, unrelated siRNA), Rab8a (100 nM), Rab8a and b (50 nM each), Rab11a (100 nM), Rab11a and b (50 nM each), and quadruple knockdown Rab8a and b, and Rab11a and b (50 nM each). (A) The cells were lysed at 48 hpt and the amount of Rab8, Rab11, and β-actin were determined by western blot analysis. (B) Intracellular ANDV N levels at 48 hpt were determined by Western blot analysis. Protein levels were normalized to GAPDH. (C) Supernatants were harvested at the time of transfection (0 h) and 48 hpt. Virus titer was determined by immune $TCID_{50}$ analysis. The fold decrease in virus titer between 0 h and 48 h was determined. Data presented is the mean of four independent experiments with duplicate wells analyzed for each condition.

lipoprotein (LDLR) (Ang et al., 2004), and polyimmunoglobulin (pIg) receptors (Apodaca et al., 1994; Rojas and Apodaca, 2002; Sheff et al., 2002). In addition to receptor recycling, the transport of select cargo from the Golgi to the plasma membrane is also regulated by this compartment (Ang et al., 2003, 2004; Chen et al., 1998; Hattula et al., 2006; Ren et al., 1998). Our model proposes a similar role for the recycling endosome in the transport of ANDV particles to the plasma membrane. Both the viral nucleocapsid and glycoproteins colocalized with eGFP-Rab8 and eGFP-Rab11 when expressed from cDNA. However, the localization of the nucleocapsid protein varied from cell to cell with some cells showing high levels of colocalization and others showing minimal colocalization. This variation seemed to be related to high nucleocapsid expression levels in some cDNA transfected cells, therefore we focused our intracellular localization studies on cells that had levels of viral protein similar to that observed in ANDV-infected cells.

The expression of constitutively active and dominant negative Rab11 proteins resulted in altered colocalization of the eGFP-fusion proteins with ANDV N during infection. The dominant negative Rab11S25N protein showed an enhanced colocalization with ANDV N, localizing closely at a perinuclear location, and is similar to observations in which Rab11S25N retained VSV G intracellularly at a perinuclear site, resulting in decreased G surface expression (Chen et al., 1998). In stark contrast to Rab11S25N, the constitutively active Rab11Q70L showed a dramatic decrease in colocalization with ANDV N. It was further determined that the two mutant Rab11 proteins localize to distinct membrane compartments. Rab11S25N localized to the *trans*-Golgi, while Rab11Q70L showed limited localization with the *trans*-Golgi marker. Consistent with Rab11 function and our model of ANDV assembly and egress, the GDP-bound mutant localizes at the donor membrane (the *trans*-Golgi) (Chen et al., 1998; Neznanov et al., 2003) and may retain or enhance ANDV N localization to that membrane compartment. In contrast the GTP-bound mutant localizes to the acceptor membrane (the recycling endosome) and by sequestering transport machinery at the recycling endosome may reduce trafficking of important host cell proteins involved in ANDV replication or trafficking of the viral proteins or particles themselves.

By utilizing RNAi, we determined that both Rab8 and Rab11 play a functional role in ANDV release from infected cells. Downregulation of Rab8a showed minimal effects on virus secretion and was similar to control transfections, however in cells transfected with siRNAs targeting Rab11a, a 10–15 fold decrease in virus secretion was observed. Downregulation both Rab11 isoforms did not enhance the effect on ANDV release seen with Rab11a downregulation alone, suggesting that Rab11a plays the predominant role in ANDV infection. In contrast, downregulating Rab8a had little effect on ANDV secretion but reducing the expression of both isoforms led to a 10-fold decrease in virus release. This result indicates that there is either redundancy in the Rab8 pathway, or Rab8b is playing a more important role in ANDV replication. It is unlikely that the effects of siRNA downregulation of Rab8 and Rab11 on virus secretion are caused by a nonspecific block in all post-Golgi secretion, since numerous studies indicate that Rab8- and Rab11-independent pathways of Golgi to plasma membrane transport exist (Chen et al., 1998; Crespo et al., 2004; Li et al., 1993; Yoshimori et al., 1996). Consistent with our model, the siRNA studies indicate an important role for Rab8 and Rab11 in ANDV replication. Given the low level of ANDV particle formation (Fig. 2), we were unable to identify the precise step at which ANDV particle egress was blocked after treatment of infected cells with Rab8 and Rab11 specific siRNAs. The siRNA sequences used were designed to recognize human forms of Rab 8 and 11 and may not be optimal for recognizing the corresponding proteins from African green monkeys. However, we utilized four siRNAs per construct and did in fact see downregulation of some Rab isoforms, indicating that siRNA downregulation of Rab transcripts was in fact occurring. A more extensive downregulation of Rab 8 and 11 protein levels may be needed to find the relatively low numbers of virus particles that are in the intracellular trafficking pathway during any particular time after ANDV infection.

Rab11a has been shown to play a role in the replication of respiratory syncytial virus (RSV) (Brock et al., 2003), HIV-1 (Murray et al., 2005; Varthakavi et al., 2006), and another retrovirus, Mason–Pfizer monkey virus (M-PMV) (Sfakianos and Hunter, 2003). In these examples, trafficking of viral proteins through the recycling endosome is required for the proteins to reach the site of particle formation at the plasma membrane, thus the recycling endosome is functioning prior to virus assembly. Although the experiments we performed have not formally ruled out a role for Rab8 and Rab11 in ANDV assembly or budding, Rab8- and Rab11-coated vesicles bud away from the membrane compartment into the cytoplasm and therefore have a different topology from that required to promote virus assembly into the Golgi lumen. Alternatively, disruption of Rab8 and Rab11 pathways could disrupt the localization of a host protein critical for virus assembly, and further studies will need to be performed to determine this possibility. Since ANDV assembly is hypothesized to occur at the Golgi, Rab8 and Rab11 are presumably altering trafficking steps that occur after virus assembly. This leads us to propose a model in which Rab8 and Rab11 are playing roles in steps of egress, downstream of virus assembly. To our knowledge, a role for the recycling endosome in post-assembly trafficking of viruses to the plasma membrane has not been described to date.

Hantaviruses may be utilizing the recycling endosome, and its function in polarized trafficking, to direct particles from the host cell in a directional fashion. Infection of polarized epithelial cells with viruses in the family *Bunyaviridae*, including ANDV, leads to the polarized release of virus particles. This release can be strictly apical, strictly basolateral, or a combination of both (Chen et al., 1991; Connolly-Andersen et al., 2007; Gerrard et al., 2002; Ravkov et al., 1997; Rowe and Pekosz, 2006) Since Rab8 and Rab11 play roles in polarized trafficking (Ang et al., 2003, 2004; Brock et al., 2003), it is possible that ANDV utilizes these pathways to egress in a polarized fashion from cells. By utilizing the recycling endosome during egress, hantaviruses could be sorted in both the apical and basolateral direction and ensure appropriate viral spread and tissue tropism within the host.

Materials and methods

Reagents and antibodies

Anti-ANDV human convalescent sera (1:150 immunofluorescence) was kindly provided by Stephen St. Jeor (University of Nevada, Reno, NV). Rabbit anti-ANDV N sera (1:500 immunofluorescence) was kindly provided by Colleen Jonsson (Southern Research Institute, Birmingham, AL). A rat anti-ANDV N sera was raised by immunizing rats with purified, bacterially expressed glutathione-S-transferase (GST)-ANDV N fusion protein (1:1500 immunofluorescence, 1:5000 western blotting and immune $TCID_{50}$, cryoelectron microscopy 1:2000). Other primary antibodies were used as follows: mouse anti-GM130 (1:100 immunofluorescence, BDBiosciences, San Jose, CA); mouse anti-Golgin97 (1:50 immunofluorescence, Molecular Probes/Invitrogen); sheep anti-TGN46 (1:250 immunofluorescence, Serotec, Oxford, UK); mouse anti-Rab8 and mouse anti-Rab11 (1:100 immunofluorescence; 1:1000 western blotting; BDBiosciences, San Jose, CA); rabbit anti-vesicular stomatitis virus glycoprotein (VSV G) (1:100 immunofluorescence, Bethyl Laboratories, Montgomery, TX); rabbit anti-glyceraldehyde-3-phosphate dehydrogenase (GAPDH) (1:1000 western blotting; Cell Signaling, Danvers, MA), and mouse anti-β-actin (1:15,000 western blotting, AbCam, Cambridge, MA). Secondary antibodies were used as follows: goat anti-rat Alexa Fluor 594, goat anti-rat Alexa Fluor 555, goat anti-mouse Alexa Fluor 488, goat anti-mouse Alexa Fluor 594, goat anti-human Alexa Fluor 633, and goat anti-rabbit Alexa Fluor 594, donkey anti-sheep Alexa Fluor 594 (1:500 immunofluorescence, Molecular Probes/Invitrogen, Carlsbad, CA); goat anti-rat horseradish peroxidase

(HRP) (1:7500 western blot, 1:5000 immune $TCID_{50}$), goat anti-mouse HRP and goat anti-rabbit HRP (1:7500 western blot, Jackson Immunoresearch, Westgrove, PA).

ANDV infection

Vero E6 cells (African green monkey kidney epithelial cells, American Type Culture Collection) were cultured as previously described and used under conditions where the cells were subconfluent and therefore not polarized (Rowe and Pekosz, 2006). Cells were infected with Andes virus, strain 9717869 (ANDV, courtesy of Stuart Nichol, Centers for Disease Control, Atlanta, GA) as previously described (Rowe and Pekosz, 2006). Infected cell supernatants were collected at the indicated times post infection or transfection and stored at −70 °C until further analysis. All infections were performed using institution-approved biosafety level 3 (BSL3) containment procedures.

Immuno-electron microscopy

For ultrastructural analysis, ANDV-infected Vero cells were fixed at the indicated days post infection in 4% paraformaldehyde, 0.1% glutaraldehyde in (Polysciences, Warrington, PA) in 100 mM PIPES, pH 7.2 with 0.5 mM $MgCl_2$ for 1 h at 4 °C. Samples were embedded in 10% gelatin and infiltrated with 2.3 M sucrose/20% polyvinyl pyrrolidone in PIPES/$MgCl_2$ overnight at 4 °C. Samples were frozen in liquid nitrogen and 70 nm sections were cut using a Leica Ultracut UCT cryo-ultramicrotome (Leica Microsystems, Bannockburn, IL). Sections were blocked with 5% fetal bovine serum and 5% goat serum (blocking buffer) for 30 min and then incubated with primary antibody for 1 h at room temperature. Sections were washed for 30 min in blocking buffer and probed with 12 nm colloidal gold-conjugated goat anti-rat secondary antibody (Jackson ImmunoResearch Laboratories, West Grove, PA) for 1 h at room temperature. Sections were washed in PIPES buffer, followed by an extensive water rinse and stained with 1% uranyl acetate and 1.6% methyl cellulose (Ted Pella, Redding, CA). Samples were visualized with a JEOL 1200EX transmission electron microscope (JEOL USA, Peabody, MA) (Beatty, 2006).

Immune $TCID_{50}$ assay

Serial 5-fold dilutions of infected cell supernatants were made in Dulbecco's modified Eagles medium (DMEM) containing 2% fetal bovine sera (FBS, Atlanta Biologicals, Atlanta, GA). Confluent monolayers of Vero cells in 96-well dishes were infected with 100 μl/well in sextuplicate. The infected cells were incubated at 37 °C, 5% CO_2 for 7 days at which time cells were washed 1× with PBS and fixed with cold 95% ethanol/5% acetic acid solution. For immunostaining, cells were rehydrated with phosphate buffered saline (PBS) and incubated in 3% bovine serum albumin (BSA, Calbiochem, San Diego, CA) in PBS (blocking buffer). Cells were incubated with rat anti-ANDV N antibody diluted in blocking buffer for 2 h at room temperature. Cells were washed with PBS and incubated with secondary antibody goat anti-rat HRP for 2 h at room temperature. Cells were washed in PBS and nucleocapsid positive wells were visualized by addition of soluble HRP substrate (DakoCytomation, Carpenteria, CA). Titers were calculated using the Reed–Muench formula (Reed and Muench, 1938).

Plasmids

The ANDV N open reading frame was amplified from ANDV vRNA and cloned into the pCAGGS (Niwa et al., 1991) and pCDNA3.1(+) (Invitrogen, Carlsbad, CA) mammalian expression vectors. Briefly, total cellular RNA was isolated from ANDV-infected Vero cells using the Qiagen cellular RNA mini prep kit according to the manufacturer's protocol (Qiagen, Valencia, CA). Using ANDV N ORF specific primers (Genebank accession: AF291702; forward primer: nucleotides (nts) 37–54 and a SacI restriction enzyme site; reverse primer: nts 1312–1330 and a SphI restriction enzyme site), the N ORF was amplified by reverse transcriptase polymerase chain reaction (RT-PCR) using Superscript One-step RT-PCR reagent (Invitrogen), digested using SacI and SphI restriction endonucleases (New England Biolabs, Ipswich, MA), and cloned into the identically digested pCAGGS vector. The ANDV N fragment was subcloned from the resulting plasmid into the pCDNA3.1(+) vector using EcoRI and XhoI restriction enzymes. The ANDV M segment ORF was amplified using M segment specific primers (Genebank accession: AF291703; forward primer: nts 46–63; reverse primer nts 3449–3469 and a KpnI restriction enzyme site), cloned into the pCR4-Blunt-TOPO vector (Invitrogen) according to the manufacturer's instructions. The M ORF fragment was excised using NotI and KpnI restriction endonucleases and this fragment was ligated to an EcoRI and KpnI digested pCAGGS vector after the EcoRI and NotI sites were blunt ended by a Klenow fill-in reaction. The sequences of both N and M ORF cDNAs were verified by DNA sequencing. The CD63-eGFP cDNA was kindly provided by David Sibley (Washington University, St. Louis, MO). The eGFP-Vps4A cDNA was kindly provided by Wes Sundquist (University of Utah, Salt Lake City, UT). The eGFP-Rab5a, eGFP-Rab7, eGFP-Rab11a, eGFP-Rab11S25N, and eGFP-Rab11Q70L, and Rab9 cDNAs were kindly provided by Phil Stahl (Washington University, St. Louis, MO). The VSV G cDNA was kindly provided by Garry Nolan (Stanford University, Palo Alto, CA). To construct the eGFP-Rab9 expression plasmid, Rab9 cDNA was amplified by PCR using canine Rab9 sequence specific primers (Genebank accession: X56386; forward primer: nts 1–28 and a XhoI restriction enzyme site; reverse primer: nts 585–606 and a KpnI restriction enzyme site) and cloned in frame with the eGFP ORF into the eGFP-C1 vector (Clontech, Mountain View, CA). The Rab8a cDNA was kindly provided by Ira Mellman (Yale University, New Haven CT). To construct N-terminal eGFP-fusions of Rab8a, canine Rab8 specific primers (Genebank accession: X56385; forward primer: nts 13–32 and containing a EcoRI restriction enzyme site; reverse primer: nts 613–633 and containing a XhoI restriction enzyme site) were used to amplify the Rab8 open reading frame by PCR before cloning into an EcoRI and SalI digested eGFP-C1 vector in frame with the eGFP ORF. The Rab8 dominant negative and constitutively active mutations were created using a four-primer PCR method. The Rab8T22N (GDP-bound) mutation was made using the following mutagenesis primers in addition to the outer primers above described to amplify the appropriate product from eGFP-Rab8wt: 5′ primer, 5′-GTGG-GGAAGAATTGTGTCCTGTTC-3′; 3′ primer, 5′-GAACAGGACA-CAATTCTTCCCCAC-3′. The Rab8Q67L (GTP-bound mutation) was made using the following mutagenesis primers: 5′ primer, 5′-CACAGCTGGTCTAGAACGGTTT-3′; 3′ primer, 5′-AAACCGTTCTAGAC-CAGCTGTG-3′. The amplified fragments were cloned into the eGFP-C1 vector. All PCR amplified products and mutations were confirmed by sequencing.

DNA transfections

Vero cells were seeded at 7.5×10^4 cells/well on coverslips in 12-well dishes one day prior to transfection. Growth media was replaced with 0.5 ml OptiMEM media (Invitrogen) prior to transfection. LT1 transfection reagent (Mirus, Madison, WI) was diluted into 100 μL of OptiMEM, mixed and incubated for 15 min at room temperature. DNA was added to the LT1 solution, mixed and incubated for 15 min at room temperature. The cells were transfected with 1 μg of DNA at a ratio of 3 μL LT1 to 1 μg of DNA. For cotransfections, 0.5 μg of each plasmid was used. The transfection mixture was added to each well, followed by 0.5 ml of growth media at 4 h post transfection (hpt). At 18–24 hpt, cells were washed 1× in PBS and fixed for 10 min in 2% paraformaldehyde in PBS. For ANDV infected cell transfections, cells

were infected at MOI = 0.5 and detached from the tissue culture dish at 72 h post infection (hpi) with 1× trypsin-EDTA. Cells were pelleted at 300 × g for 5 min, resuspended in growth media, and seeded on glass coverslips in a 12-well dish at a density of 1×10^5 cells/well. At 24 h post seeding, cells were transfected as above described.

Immunofluorescence confocal microscopy

At the indicated time post infection or transfection cells were washed with PBS and fixed in 2% paraformaldehyde in PBS for 10 min at room temperature. After fixation, cells were washed extensively with PBS and permeabilized with PBS containing 0.2% TX-100 and 0.1% sodium citrate for 10 min at room temperature. The cells were incubated with PBS containing 3% normal goat or donkey serum and 0.5% BSA (blocking buffer) for 30 min at room temperature. Cells were incubated with primary antibodies followed by secondary antibodies. All antibodies were diluted in blocking buffer and incubation times were 1 h at room temperature. Nuclei were stained with TO-PRO-3 (Molecular Probes/Invitrogen) for 15 min at room temperature. All washes were performed with PBS. Coverslips were mounted with Molecular Probes Prolong Gold antifade (Molecular Probes/Invitrogen). Cells were visualized using a Zeiss LSM 510 Meta confocal microscope. Z-stacks were acquired at a 63× magnification, 1024 × 1024 pixel resolution, using 2× digital zoom (unless otherwise noted), 0.7 μm optical slice, and 0.3 μm slice overlap.

Volocity quantitation of confocal microscopy

The amount of colocalization in the confocal z-stacks was quantitated using the Volocity (v3.0) imaging software (Improvision, Lexington, MA). Images were cropped to obtain the single cell to be quantitated. Classifiers were designed to measure three dimensional (3-D) regions according to signal intensity and region size. 3-D regions of intensity were measured using the following classifier parameters: intensity, >3 standard deviations above the mean (for eGFP signal), and >2 standard deviations above the mean for ANDV N; volume, >0.01 μm^3; separation of touching objects; and noise reduction. Classifiers were applied to measure each channel to be colocalized. The measurement calculations for each channel were colocalized using the "colocalize sessions" option to overlay the two data sets and measure the regions of colocalization. All regions less than 10 voxels were removed and the total volume of colocalization was then normalized to the total volume measured for eGFP and expressed as percent colocalization.

Small interfering RNA transfection

Small interfering RNA (siRNA) duplexes were purchased from Dharmacon (Lafayette, CO) and reconstituted at 20 μM stock concentrations according to the manufacturer's instructions. The siRNAs are designed against human Rab 8 and 11 isoforms and four siRNAs per transcript were used. Vero cells were infected in 3.5 cm^2 dishes with ANDV at MOI = 0.5 and at 72 hpi, cells were detached from the tissue culture dish with 1× trypsin-EDTA and pelleted at 300 ×g for 5 min. Cells were resuspended in growth media and seeded into 24-well dishes at a density of 5×10^4 cells/well. At 24 h post seeding (considered the 0 h timepoint), the cells were transfected with the siRNA duplexes using siQuest reagent (Mirus). For each well, 1.5 μL of siQuest reagent was diluted in 50 μL of OptiMEM media, mixed and incubated for 10 min at room temperature. The siRNAs were added to the siQuest solution at a final concentration of 50–100 nM, mixed and incubated for 30 min at room temperature. The infected-cell supernatant was harvested (0 h timepoint) and 250 μL of growth media was added to each well. The transfection mixture was added to the cells and transfections were incubated at 37 °C, 5% CO_2. Supernatants and whole cell lysates were harvested at 48 hpt. Supernatants were titered by immune $TCID_{50}$ and the fold reduction in titer was determined by dividing the titer at 0 hpt by the titer at 48 hpt (0 h $TCID_{50}$ units/ml)/(48 h $TCID_{50}$ units/ml). Virus titers were determined for duplicate siRNA transfections in four independent experiments.

SDS-PAGE and western blotting

Cells were washed once in PBS and lysed in 1% sodium dodecyl sulfate (SDS). Lysates were run through a 22-gauge needle, sonicated for 15 min, and diluted in 2× SDS loading buffer (Paterson and Lamb, 1993). Samples were boiled for 15 min and run on a 15% polyacrylamide mini gel (BioRad, Hercules, CA) at 150 volts (V) through the stacking gel followed by an additional 2 h at 100 V. Proteins were transferred to PVDF membrane (Immobilon-FL, Millipore, Billerica, MA) overnight at 22 V (Mini Transblot, BioRad). Membranes were blocked in 5% dry milk and incubated sequentially in primary and secondary antibodies for 1 h at room temperature. Washes were performed in PBS supplemented with 0.3% Tween20. HRP-conjugated secondary antibodies were detected using the ECL-Plus substrate (Amersham, Buckinghamshire, UK). Protein band intensities were quantitated by phosphorimager analysis (Fuji Film FLA3000, Tokyo, Japan).

Acknowledgments

This work was supported by Public Health Service grant R21 AI058353, The Eliasberg Foundation and The Marjorie Gilbert Foundation. We acknowledge the Molecular Microbiology Imaging Facility for technical support and all the members of the Pekosz laboratory for insightful comments and discussions.

Appendix A. Supplementary data

Supplementary data associated with this article can be found, in the online version, at doi:10.1016/j.virol.2008.09.021.

References

Ang, A.L., Folsch, H., Koivisto, U.-M., Pypaert, M., Mellman, I., 2003. The Rab8 GTPase selectively regulates AP-1B-dependent basolateral transport in polarized Madin–Darby canine kidney cells. J. Cell Biol. 163 (2), 339–350.

Ang, A.L., Taguchi, T., Francis, S., Folsch, H., Murrells, L.J., Pypaert, M., Warren, G., Mellman, I., 2004. Recycling endosomes can serve as intermediates during transport from the Golgi to the plasma membrane of MDCK cells. J. Cell Biol. 167 (3), 531–543.

Apodaca, G., Katz, L.A., Mostov, K.E., 1994. Receptor-mediated transcytosis of IgA in MDCK cells is via apical recycling endosomes. J. Cell Biol. 125 (1), 67–86.

Beatty, W.L., 2006. Trafficking from CD63-positive late endocytic multivesicular bodies is essential for intracellular development of Chlamydia trachomatis. J. Cell Sci. 119 (Pt 2), 350–359.

Brock, S.C., Goldenring, J.R., Crowe Jr, J.E., 2003. Apical recycling systems regulate directional budding of respiratory syncytial virus from polarized epithelial cells. Proc. Natl. Acad. Sci. 100 (25), 15143–15148.

Chen, S.Y., Matsuoka, Y., Compans, R.W., 1991. Assembly and polarized release of Punta Toro virus and effects of brefeldin A. J. Virol. 65 (3), 1427–1439.

Chen, W., Feng, Y., Chen, D., Wandinger-Ness, A., 1998. Rab11 is required for trans-Golgi network-to-plasma membrane transport and a preferential target for GDP dissociation inhibitor. Mol. Biol. Cell 9 (11), 3241–3257.

Connolly-Andersen, A.M., Magnusson, K.E., Mirazimi, A., 2007. Basolateral entry and release of crimean-congo hemorrhagic fever virus in polarized MDCK-1 cells. J. Virol. 81 (5), 2158–2164.

Crespo, P.M., Iglesias-Bartolome, R., Daniotti, J.L., 2004. Ganglioside GD3 traffics from the trans-Golgi network to plasma membrane by a Rab11-independent and brefeldin A-insensitive exocytic pathway. J. Biol. Chem. 279 (46), 47610–47618.

Deyde, V.M., Rizvanov, A.A., Chase, J., Otteson, E.W., St. Jeor, S.C., 2005. Interactions and trafficking of Andes and Sin Nombre hantavirus glycoproteins G1 and G2. Virology 331 (2), 307–315.

Elbashir, S.M., Harborth, J., Lendeckel, W., Yalcin, A., Weber, K., Tuschl, T., 2001. Duplexes of 21-nucleotide RNAs mediate RNA interference in cultured mammalian cells. Nature 411 (6836), 494–498.

Elliott, L.H., Ksiazek, T.G., Rollin, P.E., Spiropoulou, C., Morzunov, S., Monroe, M., Goldsmith, C., Humphrey, C., Zaki, S.R., Krebs, J.W., Maupin, G., Gage, K., Childs, J.E., Nichol, S.T., Peters, C.J., 1994. Isolation of the causative agent of hantavirus pulmonary syndrome. Am. J. Trop. Med. Hyg. 51 (1), 102–108.

Gerrard, S.R., Rollin, P.E., Nichol, S.T., 2002. Bidirectional infection and release of rift valley fever virus in polarized epithelial cells. Virology 301 (2), 226–235.
Goldsmith, C.S., Elliott, L.H., Peters, C.J., Zaki, S.R., 1995. Ultrastructural characteristics of Sin Nombre virus, causative agent of hantavirus pulmonary syndrome. Arch. Virol. 140 (12), 2107–2122.
Greaves, J., Chamberlain, L.H., 2007. Palmitoylation-dependent protein sorting. J. Cell Biol. 176 (3), 249–254.
Grosshans, B.L., Ortiz, D., Novick, P., 2006. Rabs and their effectors: Achieving specificity in membrane traffic. Proc. Natl. Acad. Sci. 103 (32), 11821–11827.
Gu, F., Crump, C.M., Thomas, G., 2001. Trans-Golgi network sorting. Cell. Mol. Life Sci. 58 (8), 1067–1084.
Hardestam, J., Klingstrom, J., Mattsson, K., Lundkvist, A., 2005. HFRS causing hantaviruses do not induce apoptosis in confluent Vero E6 and A-549 cells. J. Med. Virol. 76 (2), 234–240.
Hattula, K., Furuhjelm, J., Tikkanen, J., Tanhuanpaa, K., Laakkonen, P., Peranen, J., 2006. Characterization of the Rab8-specific membrane traffic route linked to protrusion formation. J. Cell. Sci. 119 (23), 4866–4877.
Hooper, J.W., Larsen, T., Custer, D.M., Schmaljohn, C.S., 2001. A lethal disease model for hantavirus pulmonary syndrome. Virology 289 (1), 6–14.
Hung, T., Chou, Z.Y., Zhao, T.X., Xia, S.M., Hang, C.S., 1985. Morphology and morphogenesis of viruses of hemorrhagic fever with renal syndrome (HFRS). I. Some peculiar aspects of the morphogenesis of various strains of HFRS virus. Intervirology 23 (2), 97–108.
Jantti, J., Hilden, P., Ronka, H., Makiranta, V., Keranen, S., Kuismanen, E., 1997. Immunocytochemical analysis of Uukuniemi virus budding compartments: role of the intermediate compartment and the Golgi stack in virus maturation. J. Virol. 71 (2), 1162–1172.
Jones, J.C., Turpin, E.A., Bultmann, H., Brandt, C.R., Schultz-Cherry, S., 2006. Inhibition of influenza virus infection by a novel antiviral peptide that targets viral attachment to cells. J. Virol. 80 (24), 11960–11967.
Kaukinen, P., Vaheri, A., Plyusnin, A., 2005. Hantavirus nucleocapsid protein: a multifunctional molecule with both housekeeping and ambassadorial duties. Arch. Virol. 150 (9), 1693–1713.
Ksiazek, T.G., Erdman, D., Goldsmith, C.S., Zaki, S.R., Peret, T., Emery, S., Tong, S., Urbani, C., Comer, J.A., Lim, W., Rollin, P.E., Dowell, S.F., Ling, A.-E., Humphrey, C.D., Shieh, W.J., Guarner, J., Paddock, C.D., Rota, P., Fields, B., DeRisi, J., Yang, J.-Y., Cox, N., Hughes, J.M., LeDuc, J.W., Bellini, W.J., Anderson, L.J., the SARS Working Group, 2003. A novel coronavirus associated with severe acute respiratory syndrome. N. Engl. J. Med. 348 (20), 1953–1966.
Kuismanen, E., Hedman, K., Saraste, J., Pettersson, R.F., 1982. Uukuniemi virus maturation: accumulation of virus particles and viral antigens in the Golgi complex. Mol. Cell. Biol. 2 (11), 1444–1458.
Lai, M.M.C., 2001. Coronaviridae: The viruses and their replication, In: Knipe, D.M., Howley, P.M. (Eds.), Fields Virology, fourth ed., Lippincott Williams and Wilkins, Philadelphia Pa, pp. 1163–1186.
Lai, F., Stubbs, L., Artzt, K., 1994. Molecular analysis of mouse Rab11b: A new type of mammalian YPT/Rab protein. Genomics 22 (3), 610–616.
Lau, A.S., Mruk, D.D., 2003. Rab8B GTPase and junction dynamics in the testis. Endocrinology 144 (4), 1549–1563.
LeBouder, F., Morello, E., Rimmelzwaan, G.F., Bosse, F., Pechoux, C., Delmas, B., Riteau, B., 2008. Annexin II incorporated into influenza virus particles supports virus replication by converting plasminogen into plasmin. J. Virol. 82 (14), 6820–6828.
Lee, H.W., Lee, P.W., Johnson, K.M., 1978. Isolation of the etiologic agent of Korean Hemorrhagic fever. J. Infect. Dis. 137 (3), 298–308.
Li, Y., Luo, L., Schubert, M., Wagner, R.R., Kang, C.Y., 1993. Viral liposomes released from insect cells infected with recombinant baculovirus expressing the matrix protein of vesicular stomatitis virus. J. Virol. 67 (7), 4415–4420.
Lindenbach, B.D., Rice, C.M., 2002. RNAi targeting an animal virus: News from the front. Mol. Cell 9 (5), 925–927.
Mettenleiter, T.C., 2004. Budding events in herpesvirus morphogenesis. Virus Res. 106 (2), 167–180.
Meyer, B.J., Schmaljohn, C.S., 2000. Persistent hantavirus infections: characteristics and mechanisms. Trends Microbiol. 8 (2), 61–67.
Moss, B., 2001. Poxviridae: The viruses and their replication, In: Knipe, D.M., Howley, P.M. (Eds.), Fields Virology. fourth ed., Lippincott Williams and Wilkins, Philidelphia Pa, pp. 2849–2883.
Murray, J.L., Mavrakis, M., McDonald, N.J., Yilla, M., Sheng, J., Bellini, W.J., Zhao, L., Le Doux, J.M., Shaw, M.W., Luo, C.-C., Lippincott-Schwartz, J., Sanchez, A., Rubin, D.H., Hodge, T.W., 2005. Rab9 GTPase is required for replication of human immunodeficiency virus type 1, filoviruses, and measles virus. J. Virol. 79 (18), 11742–11751.
Neznanov, N., Neznanova, L., Kondratov, R.V., Burdelya, L., Kandel, E.S., O'Rourke, D.M., Ullrich, A., Gudkov, A.V., 2003. Dominant negative form of signal-regulatory protein-alpha (SIRPalpha /SHPS-1) inhibits tumor necrosis factor-mediated apoptosis by activation of NF-kappa B. J. Biol. Chem. 278 (6), 3809–3815.
Nichol, S.T., 2001. Bunyaviruses, In: Knipe, D.M., Howley, P.M. (Eds.), Fields Virology, fourth ed., Lippincott Williams and Wilkins, Philidelphia Pa, pp. 1603–1634.
Nichol, S.T., Spiropoulou, C.F., Morzunov, S., Rollin, P.E., Ksiazek, T.G., Feldmann, H., Sanchez, A., Childs, J., Zaki, S., Peters, C.J., 1993. Genetic identification of a hantavirus associated with an outbreak of acute respiratory illness. Science 262 (5135), 914–917.
Niwa, H., Yamamura, K., Miyazaki, J., 1991. Efficient selection for high-expression transfectants with a novel eukaryotic vector. Gene 108 (2), 193–199.
Ochsenbauer-Jambor, C., Miller, D.C., Roberts, C.R., Rhee, S.S., Hunter, E., 2001. Palmitoylation of the Rous sarcoma virus transmembrane glycoprotein is required for protein stability and virus infectivity. J. Virol. 75 (23), 11544–11554.
Paterson, R.G., Lamb, R.A., 1993. The molecular biology of influenza viruses and paramyxoviruses. Molecular Virology: A Practical Approach. Oxford University Press, Oxford, U.K., pp. 35–73.
Pfeffer, S.R., 2001. Constructing a Golgi complex. J. Cell Biol. 155 (6), 873–876.
Pfeffer, S., Aivazian, D., 2004. Targeting Rab GTPases to distinct membrane compartments. Nat. Rev., Mol. Cell Biol. 5 (11), 886–896.
Ramanathan, H.N., Chung, D.H., Plane, S.J., Sztul, E., Chu, Y.K., Guttieri, M.C., McDowell, M., Ali, G., Jonsson, C.B., 2007. Dynein-dependent transport of the hantaan virus nucleocapsid protein to the endoplasmic reticulum-Golgi intermediate compartment. J. Virol. 81 (16), 8634–8647.
Ravkov, E.V., Compans, R.W., 2001. Hantavirus nucleocapsid protein is expressed as a membrane-associated protein in the perinuclear region. J. Virol. 75 (4), 1808–1815.
Ravkov, E., Nichol, S., Compans, R., 1997. Polarized entry and release in epithelial cells of Black Creek Canal virus, a New World hantavirus. J. Virol. 71 (2), 1147–1154.
Reed, L.J., Muench, H., 1938. A simple method of estimating 50 percent endpoints. Am. J. Hyg. 27, 493–499.
Ren, M., Xu, G., Zeng, J., De Lemos-Chiarandini, C., Adesnik, M., Sabatini, D.D., 1998. Hydrolysis of GTP on rab11 is required for the direct delivery of transferrin from the pericentriolar recycling compartment to the cell surface but not from sorting endosomes. Proc. Natl. Acad. Sci. U. S. A. 95 (11), 6187–6192.
Rojas, R., Apodaca, G., 2002. Immunoglobulin transport across polarized epithelial cells. Nat. Rev., Mol. Cell Biol. 3 (12), 944–955.
Roquemore, E.P., Banting, G., 1998. Efficient trafficking of TGN38 from the endosome to the trans-Golgi network requires a free hydroxyl group at position 331 in the cytosolic domain. Mol. Biol. Cell 9 (8), 2125–2144.
Rowe, R.K., Pekosz, A., 2006. Bidirectional virus secretion and nonciliated cell tropism following Andes virus infection of primary airway epithelial cell cultures. J. Virol. 80 (3), 1087–1097.
Salanueva, I.J., Novoa, R.R., Cabezas, P., Lopez-Iglesias, C., Carrascosa, J.L., Elliott, R.M., Risco, C., 2003. Polymorphism and structural maturation of Bunyamwera virus in Golgi and post-Golgi compartments. J. Virol. 77 (2), 1368–1381.
Scheiffele, P., Peranen, J., Simons, K., 1995. N-glycans as apical sorting signals in epithelial cells. Nature 378 (6552), 96–98.
Schlierf, B., Fey, G.H., Hauber, J., Hocke, G.M., Rosorius, O., 2000. Rab11b is essential for recycling of transferrin to the plasma membrane. Exp. Cell Res. 259 (1), 257–265.
Schmaljohn, C., Hjelle, B., 1997. Hantaviruses: a global disease problem. Emerg. Infect. Dis. 3 (2), 95–104.
Sfakianos, J.N., Hunter, E., 2003. M-PMV capsid transport is mediated by Env/Gag interactions at the pericentriolar recycling endosome. Traffic 4 (10), 671–680.
Sheff, D.R., Kroschewski, R., Mellman, I., 2002. Actin dependence of polarized receptor recycling in madin–darby canine kidney cell endosomes. Mol. Biol. Cell 13 (1), 262–275.
Shi, X., Elliott, R.M., 2002. Golgi localization of Hantaan virus glycoproteins requires coexpression of G1 and G2. Virology 300 (1), 31–38.
Slimane, T.A., Trugnan, G., van IJzendoorn, S.C.D., Hoekstra, D., 2003. Raft-mediated trafficking of apical resident proteins occurs in both direct and transcytotic pathways in polarized hepatic cells: Role of distinct lipid microdomains. Mol. Biol. Cell 14 (2), 611–624.
Smith, G.L., Law, M., 2004. The exit of vaccinia virus from infected cells. Virus Res. 106 (2), 189–197.
Stenmark, H., Olkkonen, V.M., 2001. The Rab GTPase family. Genome Biol. 2 (5) reviews3007.1–3007.7.
Stertz, S., Reichelt, M., Krijnse-Locker, J., Mackenzie, J., Simpson, J.C., Haller, O., Kochs, G., 2006. Interferon-induced, antiviral human MxA protein localizes to a distinct subcompartment of the smooth endoplasmic reticulum. J. Interferon Cytokine Res. 26 (9), 650–660.
Stetson, D.B., Medzhitov, R., 2006. Type I interferons in host defense. Immunity 25 (3), 373–381.
Tao, H., Xia, S.M., Chan, Z.Y., Song, G., Yanagihara, R., 1987. Morphology and morphogenesis of viruses of hemorrhagic fever with renal syndrome. II. Inclusion bodies—ultrastructural markers of hantavirus-infected cells. Intervirology 27 (1), 45–52.
Toro, J., Vega, J.D., Khan, A.S., Mills, J.N., Padula, P., Terry, W., Yadón, Z., Valderrama, R., Ellis, B.A., Pavletic, C., Cerda, R., Zaki, S., Shieh, W.J., Meyer, R., Tapia, M., Mansilla, C., Baro, M., Vergara, J.A., Concha, M., Calderon, G., Enria, D., Peters, C.J., Ksiazek, T.G., 1998. An outbreak of hantavirus pulmonary syndrome, Chile, 1997. Emerg. Infect. Dis. 4 (4), 687–694.
Varthakavi, V., Smith, R.M., Martin, K.L., Derdowski, A., Lapierre, L.A., Goldenring, J.R., Spearman, P., 2006. The pericentriolar recycling endosome plays a key role in Vpu-mediated enhancement of HIV-1 particle release. Traffic 7 (3), 298–307.
Yan, W., Frank, C.L., Korth, M.J., Sopher, B.L., Novoa, I., Ron, D., Katze, M.G., 2002. Control of PERK eIF2alpha kinase activity by the endoplasmic reticulum stress-induced molecular chaperone P58IPK. Proc. Natl. Acad. Sci. 99 (25), 15920–15925.
Yoshimori, T., Keller, P., Roth, M., Simons, K., 1996. Different biosynthetic transport routes to the plasma membrane in BHK and CHO cells. J. Cell Biol. 133 (2), 247–256.
Yoshino, A., Bieler, B.M., Harper, D.C., Cowan, D.A., Sutterwala, S., Gay, D.M., Cole, N.B., McCaffery, J.M., Marks, M.S., 2003. A role for GRIP domain proteins and/or their ligands in structure and function of the trans Golgi network. J. Cell Sci. 116 (21), 4441–4454.
Zerial, M., McBride, H., 2001. Rab proteins as membrane organizers. Nat. Rev. Mol. Cell Biol. 2 (2), 107–117.
Zhang, W., Yang, H., Kong, X., Mohapatra, S., Juan-Vergara, H.S., Hellermann, G., Behera, S., Singam, R., Lockey, R.F., Mohapatra, S.S., 2005. Inhibition of respiratory syncytial virus infection with intranasal siRNA nanoparticles targeting the viral NS1. Gene 11 (1), 56–62.